

From: Terry O'Sullivan
Sent: Friday, March 10, 2017 11:12 AM
To: Turf, Synthetic@OEHHA
Subject: Figures to accompany my public comments on crumb rubber
Attachments: RadonAdsorptionAndDesorption_v1b.pdf

Dear Advisory Panel Members,

I have previously sent a statement and 3 technical papers to Jocelyn Claude and this email address.

I am resending the statement, along with 2 figures that illustrate the large change in radon concentration (and gamma radioactivity) that occur as materials adsorb and desorb naturally-occurring radon.

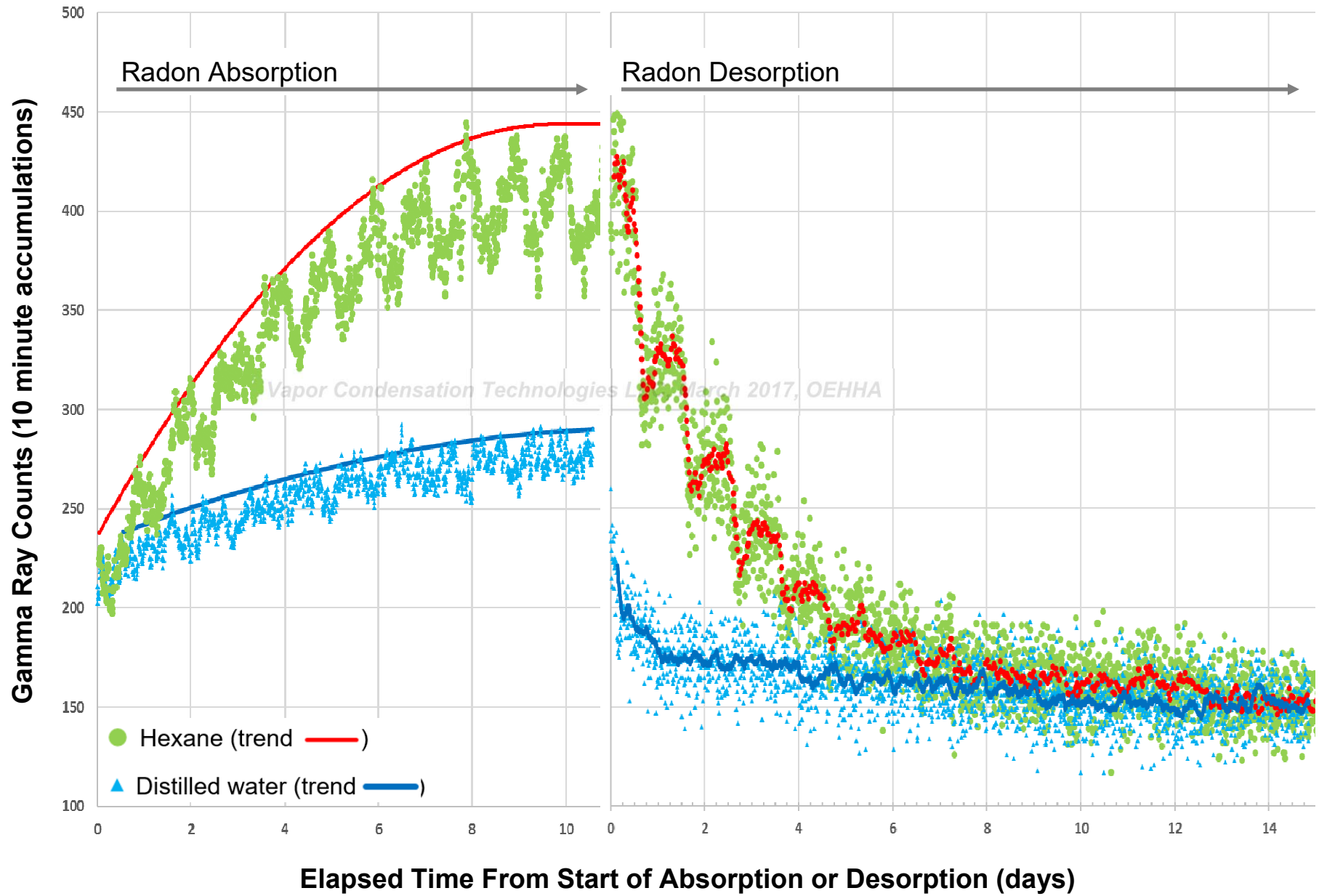
One figure compares hexane and water showing how carbon-based compounds like hexane are much more efficient at adsorbing radon.

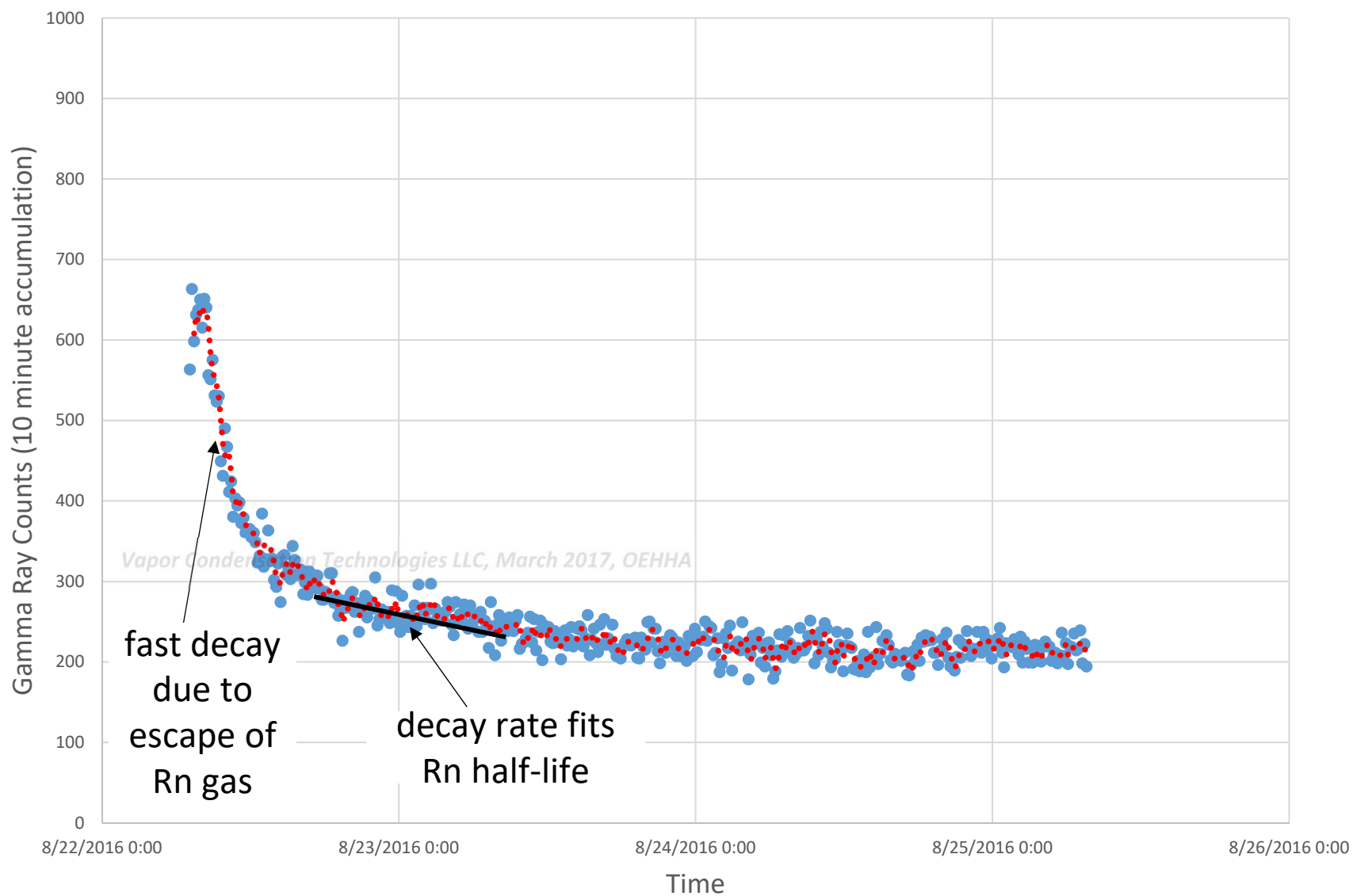
The second figure shows desorption (only) for a sample of crumb rubber.

The strong ability of a nanoporous solid like the black carbon component of crumb rubber to partition radon, suggest that, in addition to toxicity, radon adsorption and release should be studied.

Thank you.

Terry O'Sullivan





Gamma ray counts for a sample of crumb rubber, after exposure to a 50k Bq/m³ source for 12 days. The decay rate is much faster than that predicted by the radon half-life, indicating that radon is escaping from micropores.

From: Terry O'Sullivan
Sent: Friday, March 10, 2017 11:39 AM
To: Turf, Synthetic@OEHHA; Claude, Jocelyn@OEHHA
Subject: Re: Figures to accompany my public comments on crumb rubber
Attachments: CrumbRubberAdsorbsAndReleasesRadon_v1a.pdf

For your convenience, to accompany the figures I sent, here is the text of my public comments.

Thank you for your consideration.

Terry

Jocelyn Claude, Ph.D.
Associate Toxicologist
Special Investigations Section
Pesticide and Environmental Toxicology Branch
Office of Environmental Health Hazard Assessment

Dear Dr. Claude,

Thank you for the opportunity to make a brief statement to the OEHHA project staff and Scientific Advisory Panel members on the topic of artificial turf hazards.

I am petrophysicist with 35 years experience in oil, gas and geothermal energy exploration and development. For the past 20 years, I worked on steam-assisted heavy oil recovery development projects in California. During this time, I reviewed data from thousands of wells and observed large changes in gamma ray amplitude, associated with displacement of oil by steam. This led me to do additional research and to publish two papers on a phenomenon known as condensed vapor gamma or "CVG".

At its essence, CVG observes that when a cooled well at 140 degF is drilled through the 250 degF vapor cloud that remains after steam displaces heavy oil, gamma ray can be 200 times greater than expected. A few days later, gamma ray returns to normal, after the cooled well equilibrates with the hot reservoir. Cooling a cased well will cause gamma ray to increase again, and the process can be repeated. The explanation is that cooling causes vapor to condense near a cooled well, and the condensing vapor carries radon with it. The increase in gamma ray amplitude is much stronger for hydrocarbon vapor than for water vapor because radon is more soluble in carbon-based compounds than in water.

At this point, you may be asking what this has to do with artificial turf. To explain the connection, it is useful to consider the mechanism that enables activated charcoal to be used to evaluate radon concentration in basements. Activated charcoal adsorbs radon through the process of physisorption. For the CVG phenomenon, this attraction to carbon is the same mechanism that surprisingly enables radon to adsorb to, and be transported with, hydrocarbon molecules in vapor-filled rock.

The effectiveness of radon adsorption to solids has been shown to vary inversely with temperature. Noel (2015) presents data on this nanoscale adsorption process for activated carbon and other materials. At cool temperatures, and under dry conditions, more radon is adsorbed. It turns out that [carbon black](#), a component of tires that is used as a pigment and reinforcing phase, is a nanoporous material similar to activated carbon. Most importantly, carbon black can comprise 50% by of a tire (by weight). Therefore, synthetic turf made from recycled tires can concentrate radon.

For a dry playing field subject to large temperature variations, naturally-occurring radon would be adsorbed at night and released in the morning when the playing field is heated. If playing field design focuses subsurface gas release at localized areas, radon release would not only be focused in time (the morning), but also in specific areas of the playing field, for example, the goal posts of a soccer field. The process is expected to be significantly or entirely repressed for a water-saturated playing field, so wet weather could mitigate the risk of exposure.

I strongly recommend that OEHHA and the advisory panel consider that the abnormal incidence of health disorders associated with synthetic turf playing fields is related to radon partitioning and release. Evaluation of this physical phenomenon should be relatively straight forward, and experiments can be designed that would quickly lead to a conclusion.

For your reference, I have attached the three papers that I referenced. I expect to have additional papers on related topics published this year. I encourage you to support research on radon partitioning and release from synthetic turf, and I am ready to help you in any way that I can.

Best Regards,

Terence P. O'Sullivan
Vapor Condensation Technologies, LLC

Bakersfield, CA 93311

From: Terry O'Sullivan
Sent: Friday, March 10, 2017 1:18 PM
To: Turf, Synthetic@OEHHA; Claude, Jocelyn@OEHHA
Subject: Re: Figures to accompany my public comments on crumb rubber

I have 2 questions for the panel, with relation to my comments:

1. Would CAL-EPA and the committee be willing to find room to support a modest effort to further explore: a) experiments on radon adsorption and desorption by crumb rubber and associated gases, and b) field observations of radon variability (or gamma ray) on ST playing fields?
2. Does the charter of CAL-EPA allow it to study variations in radon concentration, or does this fall under the auspices of the federal government?

Thank you for the interesting presentations and your important work on analysis of ST.

Terry O'Sullivan

From: Terry O'Sullivan
Sent: Friday, March 10, 2017 1:28 PM
To: Turf, Synthetic@OEHHA; Claude, Jocelyn@OEHHA
Subject: Re: Figures to accompany my public comments on crumb rubber

Question for Dmitriy: After seeing my data on radon adsorption and release by hexane, could you envision that radon could partition to naphthalene, benzothiazole and other carbon compounds? If so, would this present an additional inhalation risk, especially under hot, dry conditions? Thank you.

Terry

From: Terry O'Sullivan
Sent: Friday, March 10, 2017 3:40 PM
To: Turf, Synthetic@OEHHA
Subject: Additional sampling unit measurements

Dr. Madellena, please also consider:

Type of rock or soil below the ST - capture samples, evaluate geology to several 100 feet below.
Measure soil water content at several depths - where is the water table?
Distance to sensor from perforations in synthetic grass surface. Number and locations of perforations.
Variations in field design.
24-7 capability for some measurements, including gamma ray!
Wind velocity and direction (you may already have this)

Thank you.

Terry O'Sullivan

HIGH GAMMA RADIATION IN HEAVY-OIL STEAM ZONES: A CONDENSATION-INDUCED EFFECT

Terence P. O'Sullivan, Aera Energy LLC

Copyright 2008, held jointly by the Society of Petrophysicists and Well Log Analysts (SPWLA) and Aera Energy LLC.

This paper was prepared for presentation at the SPWLA 49th Annual Logging Symposium held in Edinburgh, Scotland, May 25-28, 2008.

ABSTRACT

High gamma ray (**GR**), greater than 1000 GAPI, often occurs on open-hole logs through steam zones of heavy-oil reservoirs undergoing enhanced oil recovery. Days after open-hole logging, cased-hole GR through the same zones decreases to less than 100 GAPI. This extraordinary change in GR is documented and explored here.

The decrease in steam-zone GR is coincident with a wellbore temperature increase from 140°F in the mud-chilled open-hole to 250°F and higher in the stabilized cased-hole. This temperature increase occurs for both steam and hot-oil zones. However, while GR in the steam zone decreases, GR in the hot-oil zone is low in the open-hole and remains low in the cased-hole.

A conventional core through clean, well-sorted, steam- and hot-oil sands had low GR throughout and did not reveal the cause of either the high open-hole GR or the decrease in GR from open- to cased-hole. This is because the process involves a dynamic downhole mechanism, introduced here as "condensation-induced natural gamma".

Condensation-induced natural gamma derives from small amounts of naturally-occurring radon that enter the pore space in a steam zone and dissolve in droplets and vapor. High GR occurs only after circulation of cool fluid causes steam and hydrocarbon vapor to condense around the wellbore. The increase in GR arises because the concentration factor for vapor to liquid-saturated vapor or liquid usually exceeds 100:1. When the wellbore reheats, the condensate vaporizes and the effect dissipates.

The theory predicts, and experiments described here confirm, that cooling a hot well through a steam zone will regenerate high GR, and that the high GR will dissipate when the well reheats.

Condensation-induced natural gamma appears to provide a new method for identifying and characterizing condensable steam and hydrocarbon vapor.

Measuring and understanding radon adsorption in microporous materials

Raymond NOEL^{1, 2,a)}, José BUSTO^{1,b)}, Sébastien SCHAEFER³,
Alain CELZARD³, Vanessa FIERRO³

¹ CPPM, Aix-Marseille Université, CNRS/IN2P3, Marseille, France

² CINaM, Aix-Marseille Université, CNRS, Marseille, France

³ Institut Jean Lamour, UMR CNRS - Université de Lorraine n°7198, Epinal, France
On behalf of SuperNEMO collaboration

a) Corresponding author: noel@c ppm.in2p3.fr

b) busto@c ppm.in2p3.fr

Abstract. The background from the radon decay chain is the strongest constraint for many experiments working at low energy and very low counting rate. A facility for studying the optimum radon capture by very selective porous materials was developed at CPPM in the context of the SuperNEMO project. In collaboration with Institut Jean Lamour, studies were carried out for better understanding radon adsorption in carbon adsorbents.

INTRODUCTION

Radon is one of the most problematic radioactive gases for low energy and low counting experiments. It is a noble gas which belongs to the U and Th chains. Radon has typically high mobility, allowing easy escape from bulk materials and diffusion into the active parts of detectors. Later on, through successive decays, it can induce an important background in low energy physics experiments. For example, in SuperNEMO double beta decay project [1], the concentration of radon in the detector gas has to be below 150 $\mu\text{Bq}/\text{m}^3$. To reach such quite a low concentration, purifying the gas detector is required.

The only practical possibility to capture radon from a carrier gas is based on physisorption, caused by van der Waals forces at the surface of materials. However, the adsorption phenomenon corresponds to a dynamic equilibrium, as radon atoms continuously adsorb onto, and desorb from, the material's surface. The capture of radon is therefore not everlasting as its evolution from the adsorbent is only slowed down, however with a significantly decreased equilibrium partial pressure. The elapsed time between introduction and detection of radon at both ends of an adsorbent column is called "retention time". If the retention time is much larger than radon lifetime, the radon capture can be considered as complete. Temperature, pressure, adsorbent's surface area and pore-size distribution, as well as competitive adsorption of radon and carrier gas, are important parameters to be considered for the optimization of radon capture on any given material.

Activated charcoal is a well-known adsorbent, widely used for the capture of various gases [2] [3]. Activated charcoal is a highly disordered solid, presenting a quite high internal surface area and a rather broad pore-size distribution, ranging from micropores (< 2 nm) to mesopores (2 – 50 nm). In contrast, several synthetic microporous carbons materials such as carbon molecular sieves (CMS), having a much narrower pore-size distribution and hence a much higher expected selectivity with respect to radon atoms, were developed for chromatography and atmospheric chemistry applications. CMS might therefore be more suitable than activated charcoal for adsorbing radon.

In the context of the SuperNEMO collaboration, a test bench was developed at CPPM to study radon adsorption onto various microporous materials (activated charcoals, carbon molecular sieves, Metal Organic Frameworks, ...), presenting a great ability to capture radon from different carrier gases in different experimental conditions.

EXPERIMENTAL SETUP

The experimental setup is shown in Figure 1. Low amounts of radon were introduced in the carrier gas (nitrogen) by using as radon source a metal plate coated with a thin radium layer, maintained at a fixed temperature. The gas was then introduced in a buffer tank in which radon concentration, temperature, pressure and relative humidity were measured. Thereafter the carrier gas, containing a well-defined amount of radon, was introduced in the column trap located into a freezer. The saturation of the trap was measured with a commercial RAD7 radon detector, calibrated for a continuous nitrogen flow. All measurements were carried out with a flow of 10 L/h, a pressure of 1 bar and a mean radon activity of $880 \pm 23 \text{ Bq/m}^3$. The activity of the saturated column was measured by gamma spectrometry with a Ge detector using the main gamma lines of ^{214}Pb and ^{214}Bi [4].

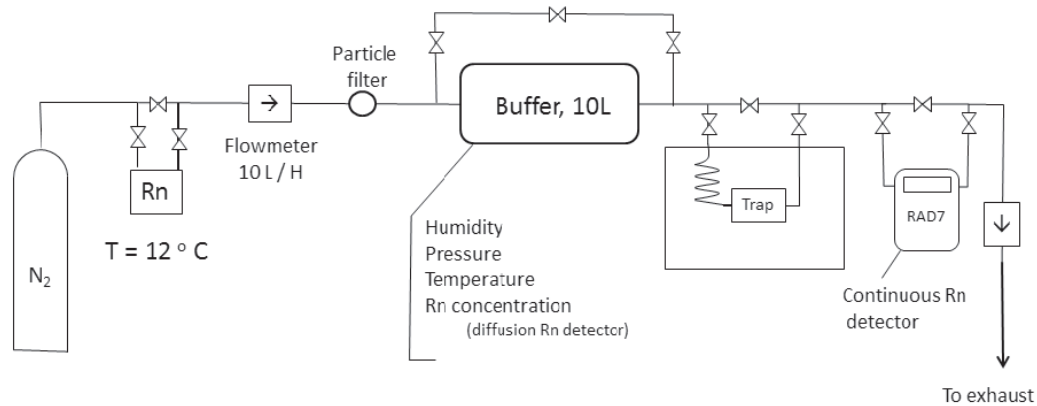


FIGURE 1. Experimental setup.

The equilibrium was assumed to be reached between radon flowing in the carrier gas and radon adsorbed in the trap when the concentration at the outlet of the trap was constant. In such conditions, the ratio of the number of radon atoms trapped to that remaining in the gas phase, both proportional to their respective activity, led to the equilibrium constant K :

$$K = \frac{\{A\}}{\{C\}} [\text{m}^3/\text{kg}]$$

where $\{A\}$ is the radon activity per unit mass (Bq/m^3) in the trap measured by the Ge detector, and $\{C\}$ is the radon activity in the gas (Bq/m^3) measured by the diffusion radon detector.

ADSORBENT MATERIALS TESTED

Only adsorbents having high surface areas and relatively low specific radioactivities were considered in the present work. Nevertheless, in order to better understand the radon adsorption phenomenon, studying standard zeolites and other materials also presenting a great potential for radon capture is foreseen in the near future, even if they present a too high intrinsic radioactivity for the SuperNEMO experiment.

The materials selected for this preliminary study were, see Table I:

- classical activated charcoals (K48 special¹, K48¹, NuclearCarb², Envirocarb², G2X4³), characterized by high surface areas and broad pore-size distributions;

¹ Classical activated carbon from Sillicarbon

² Classical activated carbon from Chemviron Carbon

³ Classical activated carbon from Japan EnviroChemicals

- carbon molecular sieves (Carbosieve SIII⁴, Carboxen 1000⁴, and 569⁴), characterized by well-defined, narrower, pore sizes;
- synthetic carbon (Carboact⁵), widely used in low background experiments.

TABLE I. Radon adsorption K-factor parameter for several adsorbents investigated at 20°C, 0°C, -30°C, and -50°C.

Sample	K factor at 20°C (m ³ /Kg)	K factor at 0°C (m ³ /Kg)	K factor at - 30°C (m ³ /Kg)	K factor at - 50°C (m ³ /Kg)
K48	13 ± 1.5	14 ± 1.5	77 ± 6.9	232 ± 20
K48S	11 ± 1.2	19 ± 2.0	69 ± 6.1	276 ± 23
G2X4	6.3 ± 0.7	24 ± 2.6	69 ± 6.1	253 ± 22
NUCLEARCARB 208C 5KI3	7 ± 0.8	15 ± 1.6	55 ± 4.9	190 ± 16
NUCLEARCARB 208C 5TEDA	3.9 ± 0.4	11 ± 1.2	40 ± 3.6	170 ± 14
ENVIRONCARB 207C	13 ± 1.5	21 ± 2.2	101 ± 9.0	270 ± 23
Carboact	17.1 ± 1.9	36 ± 3.9	182 ± 16.2	480 ± 41
carboxen 1000	11.4 ± 1.3	35 ± 3.7	148 ± 13.2	484 ± 41
carboxen 569	2.2 ± 0.2	7.8 ± 0.8	14 ± 1.2	100 ± 9
carbosieve SIII	16.5 ± 1.9	68 ± 7.3	160 ± 14.2	518 ± 44

Table 1 shows the K-factor for ten samples measured at 20°C, 0°C, -30°C and -50°C. As it can be seen, carbon molecular sieves (especially Carbosieve III and Carboxen 1000) presented a high affinity for radon at low temperatures (-50°C), much higher than that of standard charcoals. This advantage, however, decreased when the temperature increased, so that the adsorption capacity of carbon molecular sieves at room temperature was similar to that of the best activated charcoals.

ADSORPTION ANALYSIS

A series of charcoals and carbon molecular sieves were investigated at Institut Jean Lamour. N₂ and CO₂ adsorption-desorption isotherms were measured for each material. From these data, the corresponding pore-size distributions (PSDs) were obtained. As an example, Figure 2 shows the PSDs of K48 charcoal and Carbosieve SIII samples. As expected, CMSs have narrower PSDs than regular charcoals.

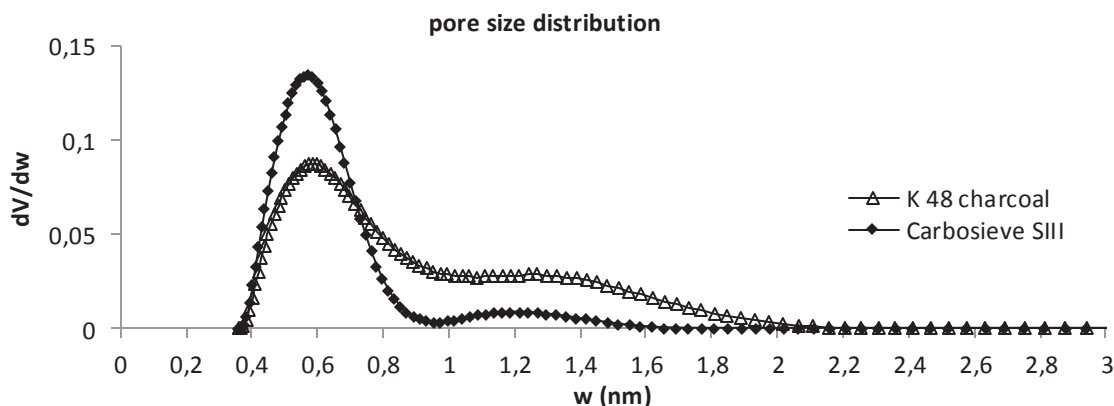


FIGURE 2. Pore size distributions of a standard charcoal and a carbon molecular sieve.

⁴ Carbon Molecular Sieve from Supelco, Inc.

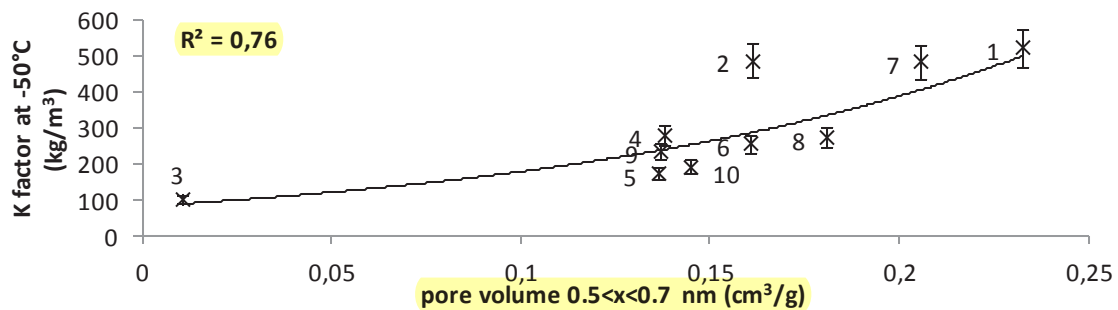
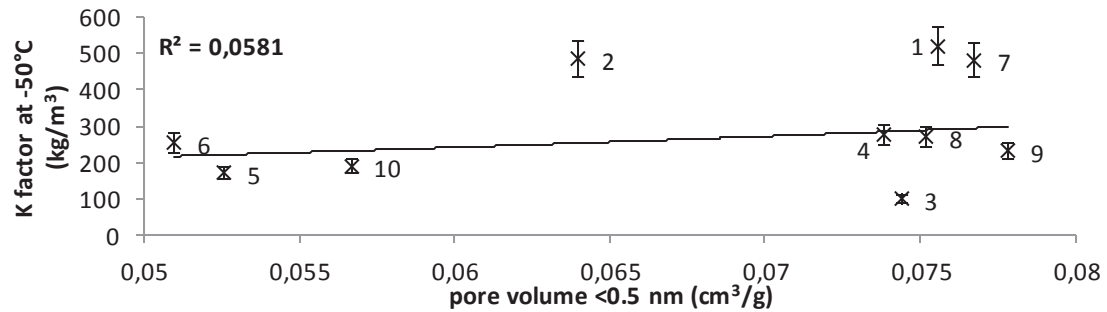
⁵ Synthetic activated charcoal from Carboact

The PSDs were used to calculate the cumulated pore volume in several pore size intervals: < 0.5 nm, between 0.5 and 0.7 nm, < 0.7 nm (ultramicropores), between 0.7 and 2 nm (supermicropores), < 2 nm (micropores) and above 2 nm (mesopores).see table II

TABLE II. Textural analysis of material used

Sample	Surface area BET (m ² /g)	Pore volume <0.5 nm (cm ³ /g)	pore volume <0.7 nm (cm ³ /g)	pore volume 0.5-0.7 nm (cm ³ /g)	pore volume 0.7-2 nm (cm ³ /g)	pore volume <2 nm (cm ³ /g)
K48	793	0.078	0.215	0.137	0.099	0.314
K48S	799	0.074	0.212	0.138	0.105	0.317
G2X4	1383	0.051	0.212	0.161	0.322	0.534
NUCLEARCARB 5KI3	1315	0.057	0.202	0.145	0.321	0.522
NUCLEARCARB 5TEDA	1297	0.053	0.189	0.137	0.321	0.510
ENVIRONCARB 207C	1073	0.075	0.256	0.181	0.165	0.421
Carboact	1096	0.077	0.283	0.206	0.156	0.439
carboxen 1000	812	0.064	0.225	0.161	0.045	0.270
carboxen 569	299	0.074	0.085	0.011	0.000	0.085
carbosieve SIII	1061	0.076	0.308	0.233	0.102	0.410

The objective was to find a relationship between pore diameter and radon adsorption. Thus, the K-factor was plotted as a function of pore volume for each range of considered pore diameters.



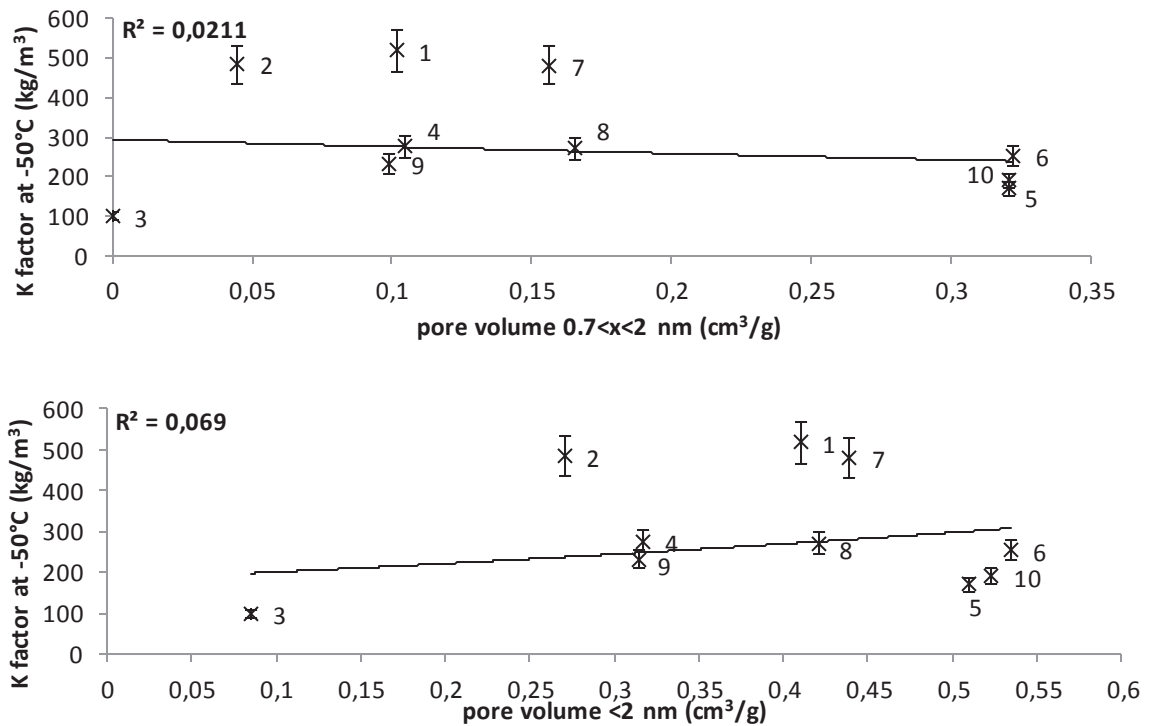


FIGURE 3. Radon adsorption K-factor measured at -50°C , as a function of cumulated pore volume (for pore diameters below 0.5 nm, ranging from 0.5 to 0.7 nm, ranging from 0.7 to 2 nm and below 2 nm), for several samples (1: Carbosieve III; 2: Carboxen 1000; 3: Carboxen 569; 4: K48S; 5: Nucleacarb 208C-5TEDA; 6: G2X4; 7: Carboact; 8: environcarb_207; 9: K48; 10: Nucleacarb 208C 5KI3). The lines are exponential fits to the experimental data.

The micropore volume (< 2 nm) was not found to be correlated with the K-factor. But a clear trend between K-factor and cumulated volume of pores with diameters ranging from 0.5 to 0.7 nm was observed, as shown in Figure 3. The PSD thus seems to be an important parameter for selecting materials having the highest radon adsorption capacity. Except for a few samples, the values of K-factor were indeed correctly fitted by an exponential law, R^2 being the correlation parameter. The same correlation was always seen, whatever the adsorption temperature. This finding suggests that radon is preferentially adsorbed in this range of pores, and that physisorption is the main contribution to radon adsorption. However, heteroatoms, ashes or surface functionalities might also affect radon-carbon interactions and explain deviations.

CONCLUSION

In the context of the SuperNEMO collaboration, a facility to study and optimize radon adsorption on porous materials was built. Several measurements based on commercial microporous carbon materials were carried out, from which very important information on the radon adsorption process was obtained. A better understanding of radon adsorption properties of carbon materials is now to be expected. Extending our work to different carrier gases is also planned in the near future.

REFERENCES

- [1] R. Arnold et al., *Eur. Phys. J.* **C70** 927-943 (2010).
- [2] S. C. Scarpitta, *Health Physics* **62**, 576 (1992).
- [3] W. C. Gaul, PhD Thesis, University of Carolina (2003).
- [4] K. P. Strong et al., *15th DOE nuclear air cleaning conference*, 627 (1978).

Measuring and understanding radon adsorption in microporous materials

Raymond Noel, José Busto, Sébastien Schaefer, Alain Celzard, and Vanessa Fierro

Citation: *AIP Conference Proceedings* **1672**, 070001 (2015); doi: 10.1063/1.4927992

View online: <http://dx.doi.org/10.1063/1.4927992>

View Table of Contents: <http://scitation.aip.org/content/aip/proceeding/aipcp/1672?ver=pdfcov>

Published by the *AIP Publishing*

Articles you may be interested in

[Construction and measurements of a vacuum-swing-adsorption radon-mitigation system](#)

AIP Conf. Proc. **1549**, 116 (2013); 10.1063/1.4818089

[Radon adsorption in nanoporous carbon materials](#)

AIP Conf. Proc. **1549**, 112 (2013); 10.1063/1.4818088

[Effective interactions in multisite cells for adsorption in microporous materials](#)

J. Chem. Phys. **130**, 164701 (2009); 10.1063/1.3114445

[A locally analytic density functional theory describing adsorption and condensation in microporous materials](#)

J. Chem. Phys. **108**, 1162 (1998); 10.1063/1.475479

[Adsorption of polymeric fluids in microporous materials. I. Ideal freely jointed chains](#)

J. Chem. Phys. **99**, 8325 (1993); 10.1063/1.465605

In-Situ Evaluation of Vapor Properties Using Condensed Vapor Gamma¹

Terence P. O’Sullivan²

ABSTRACT

Gamma-ray (GR) logs from infill wells in heavy-oil development projects frequently exceed 1,000 GAPI, but only through the hot vapor cloud that develops as injected steam displaces heavy oil. GR values in the same sands that are liquid-filled, and immediately below the vapor-filled rock, are typically less than 100 GAPI. Previous work showed that high GR values are caused by drilling-related cooling of vapor-filled rock. Gamma-ray values are thought to increase when water and hydrocarbon molecules approach the dewpoint and condense around a chilled well. As solubilized radon concentrates in these droplets, GR values can increase by $\geq 100x$. After the chilled well begins to reheat and equilibrate with the hot reservoir (36 hours or less) GR values return to normal levels. An experiment demonstrated that the cycle of GR increase and decrease can be repeated indefinitely, simply by chilling the well and then allowing it to warm back.

To put the condensed vapor gamma (CVG) effect into context, logs from thousands of heavy-oil development wells from two large oil fields of the San Joaquin Valley, California, were systematically reviewed.

The observations suggest that it is possible to develop a method for in-situ evaluation of vapor properties. Although the condensation-induced gamma signal has only been documented to occur in wells drilled in heavy-oil steamfloods, the effect could occur in any reservoir containing condensable vapor, provided that the vapor can be cooled to the dewpoint.

Controlled generation of CVG in the laboratory is a logical next step toward improved understanding of this phenomenon. Continuous in-situ observation and monitoring of CVG is also recommended in order to explore the linkage between CVG and development activities.

INTRODUCTION

Heavy-oil reservoirs in the San Joaquin Valley, California, have been developed with cyclic and continuous steam injection since the 1960s. Reservoirs in these giant oil fields consist of massive sands, up to 600-ft thick, that are part of fluviodeltaic and turbidite sequences. Quartz and plagioclase feldspar comprise $\geq 75\%$ or more of these rocks, and clay content is typically $< 5\%$. Average porosity for these clean sands is 25 to 35%, and permeability is generally greater than 1,000 mD, but the oil is heavy, with a typical gravity of 12° API. Thousands of vertical wells have been drilled to implement the steamflood process, typically with total depth $< 2,000$ ft, and interwell spacings that can be < 200 ft.

Prior to steam injection, logs show that natural gamma-ray (GR) values in oil-saturated reservoir rock are < 100 GAPI. After steam displaces the heavy oil, these clean sands contain hot vapor and a small amount of residual oil and water. Surprisingly, when this steamflooded interval is

logged in new wells targeting deeper reserves (Fig. 1), GR logs often measure values $> 1,000$ GAPI.

This phenomenon is only seen through hot, vapor-filled intervals, and only while a well remains cool as a result of circulating chilled mud during the drilling process. In Well A of Fig. 1, the cased-hole GR log (blue curve) was run 10 hours after the openhole GR log, while wellbore temperature remained below 200°F (temperature logs in Track 3) and under this condition, the high GR values repeated. In Well B, however, the cased-well was logged 36 hours after openhole logging, when the well had reheated to 250°F. This time, the GR values had decreased below 100 GAPI. Previous work (O’Sullivan, 2008) demonstrates that the high gamma values can be regenerated by circulating water and cooling a cased well to 100°F. Spectral gamma-ray data show that the high GR values are primarily due to the uranium series.

The best explanation for these high-amplitude and controllable variations in GR values is provided by the process of condensed vapor gamma (CVG) (O’Sullivan, 2009). The process begins when water and hydrocarbon

Manuscript received by the Editor on July 22, 2015; Revised manuscript received on August 11, 2015.

¹Originally presented at the SPWLA 56th Annual Logging Symposium, Long Beach, California, USA, July 18-22, 2015, Paper LLL.

²Aera Energy LLC, Bakersfield, CA, 93311, USA; Email: tposullivan@aeraenergy.com

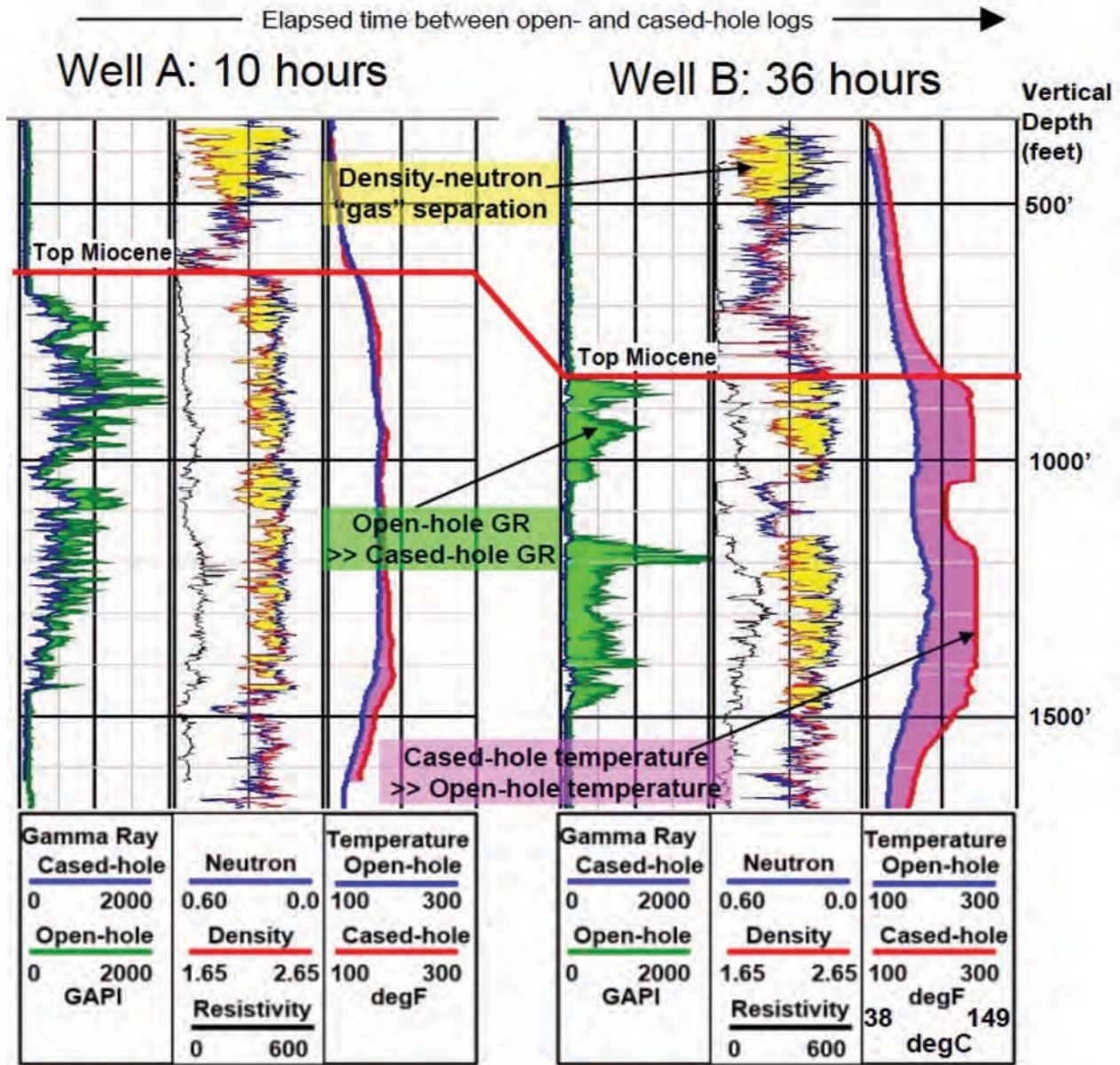


Fig. 1—High gamma-ray (GR) on openhole logs through hot, vapor-filled rock repeats on the cased-hole log for Well A, but not for Well B. Cased-hole logs for Well A were run only 10 hours after the openhole logs, while the wellbore temperature was still <200°F. For Well B, cased-hole temperature has equilibrated with the hot reservoir, and the GR log reads normal values of ≤100 GAPI.

molecules in the hot vapor cloud are pulled toward a chilled wellbore where vapor is condensing. At the wellbore, radon is concentrated in droplets of condensed vapor and radioactive decay produces the daughter products that generate the high gamma. The CVG signal decreases when the wellbore reheats and the droplets vaporize.

Several aspects of CVG are explored further in this paper, including the factors that influence the magnitude of CVG, and observations of the spatial and temporal patterns of CVG occurrence. Under certain conditions, CVG may provide an in-situ method for evaluation of vapor properties.

OBSERVATIONS OF CVG AMPLITUDE

Figure 2 contains multiwell log displays for intervals of two Midway-Sunset reservoirs that have been steamflooded. Reservoir 1 (Fig. 2a) is dominated by clean, well-sorted sands whereas Reservoir 2 (Fig. 2b) is dominated by poorly sorted sands (with the exception of the well-sorted Sand 2A). Each display shows a combined interval of ~500 ft from several wells with the well boundaries shown by the color changes in the resistivity track. The core photos show representative intervals of each reservoir, taken from nearby

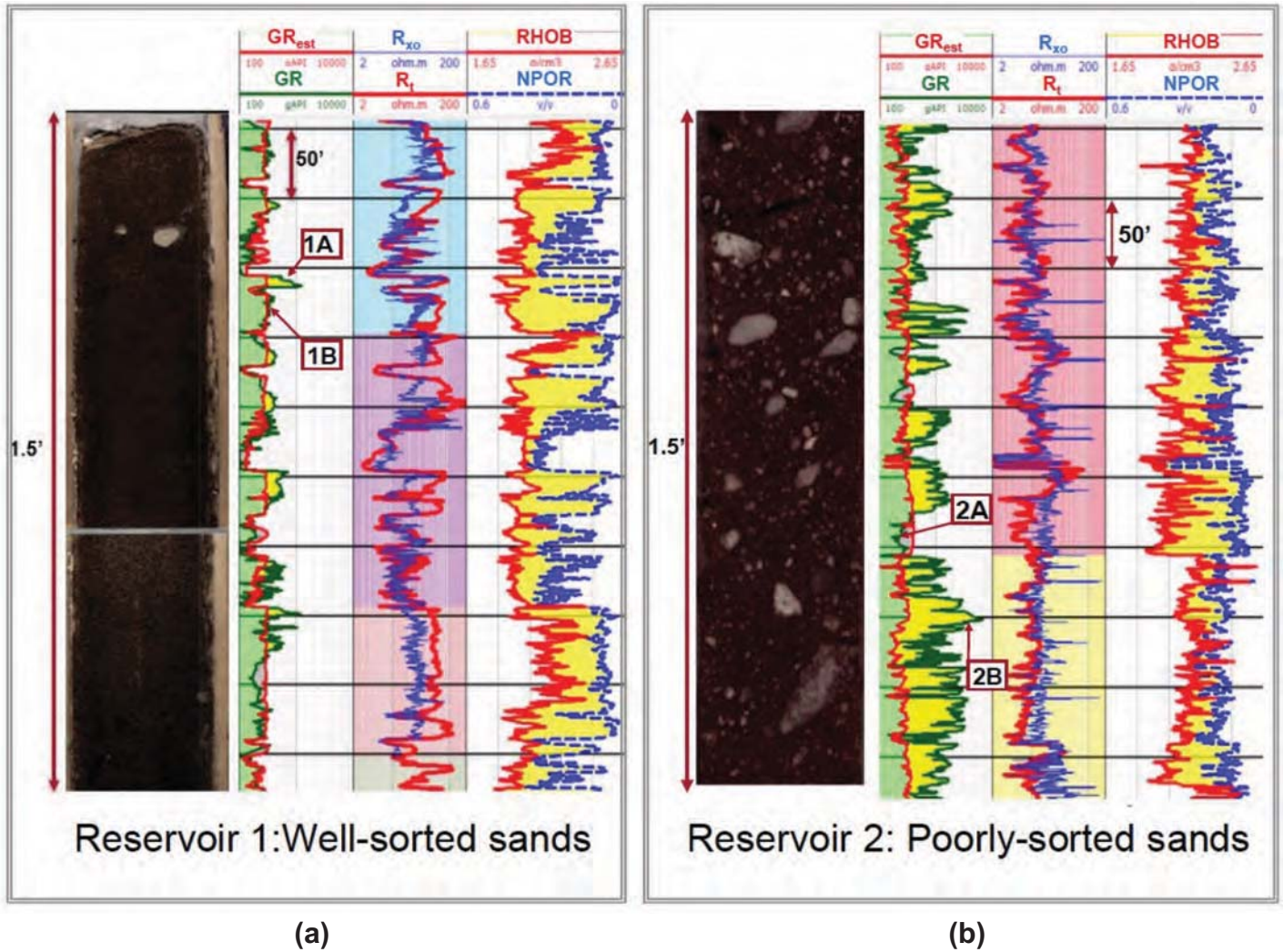


Fig. 2—Log responses for steamflooded reservoirs at Midway-Sunset. Photos are for 18-in. intervals of oil-saturated core, taken from nearby wells, prior to steamflooding. For a steamflooded reservoir, the GR log is significantly higher than GR_{est} for poorly sorted rock with higher residual oil saturation (S_{or}). GR_{est} is simply a baseline estimate of GR, based on density, neutron and resistivity data from intervals with <300 GAPI, where CVG is minimal or absent. (a) The well-log display for Reservoir 1 (well-sorted sands) shows data from four wells, with boundaries shown by color change; (b) the well-log display for Reservoir 2 (poorly sorted sands) shows two wells, with boundaries shown by color change.

wells prior to steamflooding.

To facilitate comparison between wells, estimated GR baseline values (GR_{est}) were generated by selecting intervals from wells with GR values <300 GAPI. The 300-GAPI cutoff is intended to limit the selected intervals to liquid-filled rock where CVG is minimal or absent. For these intervals, multiple regression was used to generate GR_{est} from density, neutron and resistivity data. GR_{est} simply provides a reference that can be used to locate intervals with the unusually high GR values that characterizes the CVG response.

The observed GR values are plotted in the left track as the green curve, on a log scale from 100 to 10,000 GAPI, with yellow shading to GR_{est} . Comparing the GR log and other logs in Figure 2 we see that

1. Density-neutron curve separation is larger for the well-sorted sands in Reservoir 1 and interval 2A of Reservoir 2.
2. Resistivity curve separation (from R_t to R_{xo}) is lower in poorly sorted sands, and the resistivity is smoother and less blocky.
3. Observed GR log is consistent with the estimated GR log for well-sorted sands, but much higher than the estimated GR log for poorly sorted sands (e.g., Sand 2B). Overall, the GR log is much higher for the poorly sorted sands.
4. For well-sorted Sands 1A and 1B, there is no apparent change that explains the increase in GR log from 300 GAPI in Sand 1B, to more than 1,150 GAPI in Sand 1A, over a distance of just a few feet.

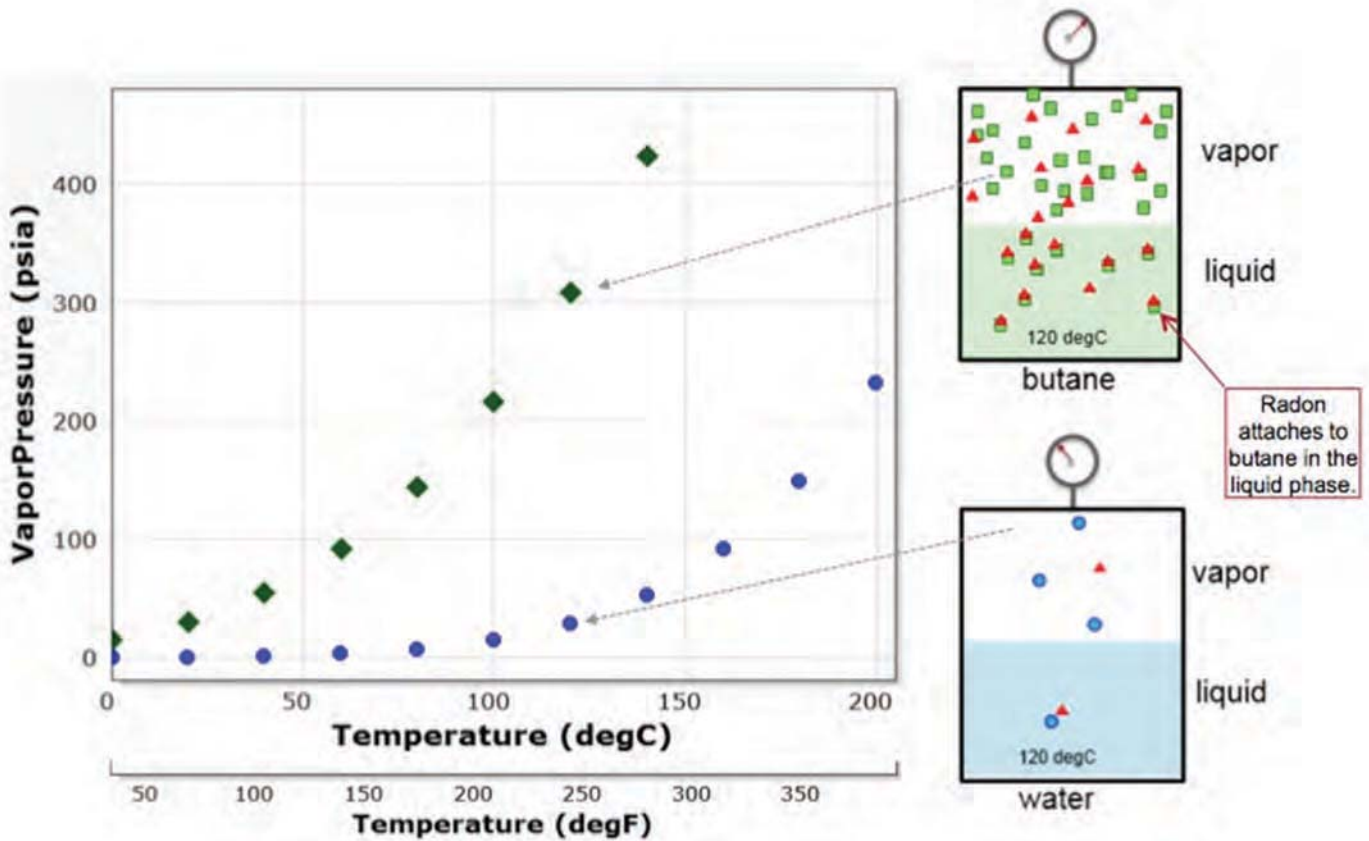


Fig. 3—Vapor pressure vs. temperature, and schematics for closed-cell experiments on butane and water. For a given temperature, vapor pressure is higher for butane than water. At 120°C, butane molecules are ~10x more abundant than water in the vapor phase. For the butane cell, 10x higher solubility of radon (red triangles) in hydrocarbon than in water leads to a10x higher partial pressure of radon in the butane vapor phase. When droplets of condensed vapor form around a cooled wellbore, they solubilize energetic radon from the vapor cloud, occasionally concentrating it by a factor ≥200.

The differences in density-neutron and resistivity curve separation, described in Items 1 and 2 above, are classical features that differentiate well-sorted from poorly sorted reservoirs. The difference in GR (Item 3) is unexpected, and has to do with lower sweep efficiency, and higher residual oil saturation, for the more poorly sorted sands. The GR increase from Sand 1B to Sand 1A (Item 4) will also be explained as related to the influence of hydrocarbon.

FACTORS THAT INFLUENCE CVG AMPLITUDE

From the current understanding of the CVG mechanism, the factors that influence CVG amplitude can be separated into four groups:

1. Drilling-related properties, including wellbore temperature, cumulative cooling time and elapsed time since buildup.
2. Reservoir properties, including pressure and

temperature.

3. Rock properties, including intrinsic radioactivity, porosity, and relative permeability.
4. Liquid- and vapor-phase properties, including oil and water saturation, solubility of radon, oil composition, and vapor pressure.

For the reasons below, Group 4 contains the factors that are most likely to have a degree of vertical variability that could be linked to the kind of change in GR values that is seen from Sand 1B to Sand 1A.

For Group 1, lost circulation rarely occurs while drilling through these reservoirs and abrupt changes in GR amplitude for intervals <10-ft thick are unlikely to be explained by lost circulation. Examples discussed later in this paper show that high GR responses correlate between closely spaced wells and persist for years. Lost circulation is unlikely to occur identically for groups of wells.

For Group 2, observed pressure and temperature variations from openhole formation pressure tests and cased-hole formation temperature surveys, vary slowly with depth and cannot explain the abrupt variations in GR values.

For Group 3, intrinsic radioactivity for liquid-filled sands and shales is <300 GAPI. CVG responses in vapor-filled reservoirs (described later in this report) can exceed 20,000 GAPI over 100 ft or more, and are not due to lithology because core samples through high-GR intervals (O'Sullivan, 2008) have GR values <300 GAPI, and an experiment demonstrated that the high GR log is a temporary effect related to wellbore cooling.

By the process of elimination, assuming that the four groups completely describe all possible factors, it appears that the changes needed to explain large variations in CVG through vapor-filled rock are most likely to originate from variations in Group 4, the vapor-phase properties. In this light, the inability of the conventional log data to explain the reason for the difference between the GR log in Sands 1A and 1B is understandable. Conventional log measurements respond weakly, or not at all, to vapor properties, so they show no correlation with CVG signal amplitude.

This line of reasoning is worth pursuing, because published data (UNSCEAR, 1982; Gross et al., 1999; Al-Azmi, 2004) indicate that radon is significantly more soluble in oil than in water.

Kharaka, et al. (1988) measured the solubility of noble gases in crude oil from the Elk Hills oil field, in the San Joaquin Valley, California. Measurements were made for He, Ne, Ar, Kr and Xe. They found that solubility increases with atomic mass, and with higher API gravity oil. Compared to pure water, they found that Xe (atomic mass of 133, compared to 222 for Rn) is 24x more soluble in crude oil. Compared to 350,000-ppm brine, Xe is 300x more soluble in crude oil. Rn solubility was not measured, but the correlation with atomic mass strongly suggests that Rn solubility in oil would be higher than that of Xe.

The high solubility of radon in oil is an outcome of the "like-dissolves-like" rule. That is, nonpolar radon tends to "stick" to nonpolar hydrocarbon more than water.

Solubility is important because Henry's law (Battino and Clever, 1966) states that the partial pressure of a gas in equilibrium with a solvent is directly proportional to the solubility of the gas in the solvent. Therefore, if radon is 20x more soluble in oil than water, the concentration of radon in oil vapor is approximately 20x greater than the concentration in water vapor. (An exact multiple of 20x requires that ideal gas law for partial pressure of radon is precisely adhered to.)

Together with solubility, vapor pressure influences the composition of the vapor cloud, especially when the hydrocarbon phase contains low-boiling point hydrocarbons

like butane (0°C, 32°F). The crossplot in Fig. 3 shows how the equilibrium vapor pressure increases with increasing temperature for water and butane. In Fig 3, the schematics at right are a snapshot of a conceptual experiment. At this time, both cells are at 120°C (248°F). One of these closed cells is half-filled with liquid water, the other half-filled with liquid butane. In the butane cell, the vapor pressure is >300 psia, compared to 30 psia for the water cell.

In the liquid phase, both cells also contain radon (red triangles) in proportion to solubility, using a conservative 10:1 oil-to-water radon solubility ratio. For simplicity, all the radon is solubilized in either butane (green) or water (blue) molecules. In the butane liquid phase, 10 of 30 butane molecules are tagged with radon, compared to only 1 of 30 molecules in the liquid phase of the water cell. (In reality, at 100 GAPI, the liquid phase will be well-undersaturated with respect to radon, but the butane:water ratio remains the same.) The solid blue and green colors of the water and butane phases, respectively, signifies that there are many more molecules, in addition to the tagged molecules.

In the vapor phase at 120°C (248°F), where the greatly reduced molecular density is proportional to vapor pressure, there are 30 butane vapor molecules for every 3 water vapor molecules in the water cell. The higher solubility of radon in butane (10x) means that (compared to water) there are also 10x more radon atoms in the vapor phase of the butane cell, but due to the high free energy of the vapor phase these radon atoms are not tightly linked to butane (or water) molecules. In the vapor cloud, the partitioned radon only becomes concentrated when liquid droplets form near a chilled wellbore. Solubility, and the proximity of droplets to the logging tool, increases GR values for both water and hydrocarbon. However, compared to water droplets, which may yield GR values of 250 GAPI, the higher solubility of radon in hydrocarbon apparently drives the GR log to values of $\geq 25,000$ GAPI.

When present in some sands and absent in others, this is how light hydrocarbons build the potential for high-amplitude variations in GR values, for example, that seen for intervals 1A and 1B in Fig. 2.

It is important to note that the measured GR values do not increase above the intrinsic GR values (i.e. the value for the liquid-filled rock) until the temperature around a chilled well, through an interval containing hot vapor, approaches the dewpoint and droplets begin to form. Condensation provides the essential multiplier that temporarily increases GR values.

CAN CVG BE MAPPED?

For CVG to provide a useful reservoir surveillance tool, the response needs to be spatially coherent, and variations through time should be connected to development activities. To determine if this is happens, and to put the CVG response into context, logs from thousands of heavy-oil development wells from two large oil fields of the San Joaquin Valley, California were systematically reviewed.

For a reservoir in Midway-Sunset Field, the average GR reading was mapped for intervals of wells with GR values >300 GAPI (considerably higher than GR reading in shale). The map in Fig. 4 shows patterns that are encouraging. For this turbidite reservoir, the low gamma-ray values (yellow/green) occur in a well-sorted facies, and the high GR values (red) are associated with a more poorly sorted facies. The pattern of response and amplitude variation fits well with the responses discussed in relation to the well-sorted and poorly sorted reservoirs in Fig. 2.

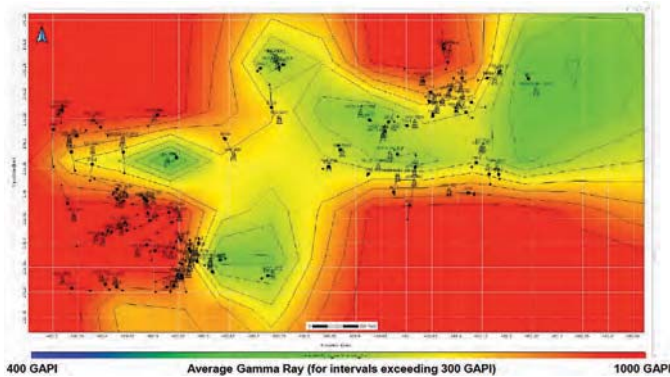


Fig. 4—For intervals with GR values >300 GAPI, a map of average GR values for a reservoir at Midway-Sunset field shows systematic variations. Higher GR values occurs in poorly sorted rock, because radon is more soluble in oil than water, and residual oil is higher in poorly sorted rock. The yellow and green colors, representing lower GR, suggest a well-sorted channel.

Following this “success”, logs from 5,500 wells in Belridge Field were culled to select wells with high GR values. The interval of interest is the Tulare Sand, which was developed as a heavy-oil steamflood starting in the 1980s. For this reservoir, over 1,000 wells were found to have GR readings >1,000 GAPI, and 231 wells had GR readings >2,000 GAPI. Logs from four wells with GR readings >10,000 GAPI are shown in Fig. 5.

BULK-DENSITY ANOMALIES

For the wells in Fig. 5, Track 1 shows the openhole GR log on a logarithmic scale from 100 to 20,000 GAPI, and Track 4 shows the bulk-density, scaled from 1 to 6 g/cm³. The unusual bulk density scale in Track 4 is needed to display the extreme range of bulk-density values for these wells. The

high bulk-density values only occur in intervals with very high CVG values >5,000 GAPI. The high GR response is beyond calibration limits, so the accuracy may decrease, but the measurement does reflect downhole conditions. The high bulk density is suspicious-looking.

As shown by the yellow-shaded area in Fig. 6, the cause is related to natural gamma “spillover” into the density detector range. For a normal GR spectra, only a small and insignificant amount of energy (blue shading) falls within the density detector range. This changes at high natural GR amplitudes, when much more GR energy falls within the density detector range and gamma counts increase.

At very high counting rates, one problem with the density tool occurs because of limits to detector electronics, commonly referred to as dead time. Normally, as each pulse is detected and processed, there is a small time during which others cannot be detected. There is a correction for this effect, but it only works for modest ranges of counting rates. A second problem occurs because of pile up at the detector, when a large number of gamma rays arrives during the time of a single, normal pulse. The probability for this to happen increases exponentially with increasing gamma-ray detection rate. When this occurs, the amplitudes of the more or less coincident pulses add, and the multiples are detected as a single count of enormous energy (Ellis, 2013, personal communication).

These problems combine to cause detector paralysis, resulting in low or zero count rates, and translating into very high, and false, readings of apparent bulk density. The density log response is an artifact, but the GR response is real, and requires closer examination.

SPATIAL CORRELATION

Figure 7 is a cross section based on seven closely spaced wells drilled through the Tulare Sand to a deeper reservoir, after the Tulare steamflood had recovered most of the oil. Well A was drilled in the year 2000, and Well E was drilled in 2004. The remaining five wells were drilled in 2008. The inset map shows that interwell spacings are <250 ft.

GR values, plotted on a log scale from 100 to 10,000 GAPI, are >1,000 GAPI in all seven wells, and approach or exceed 10,000 GAPI in Wells F and G. The high amplitude of the GR values is remarkable, and the correlation between wells over a 60-ft interval, and a span of eight years, continues to demonstrate that CVG is a reservoir-scale property with high signal-to-noise and long duration. There is an interesting problem with these high GR values, however.

Remaining oil saturation in these sands, following steam injection that began in the 1980s is very low. Based on the CVG amplitudes for well-sorted and poorly sorted sands (Fig. 2), the GR amplitude through these sands is expected

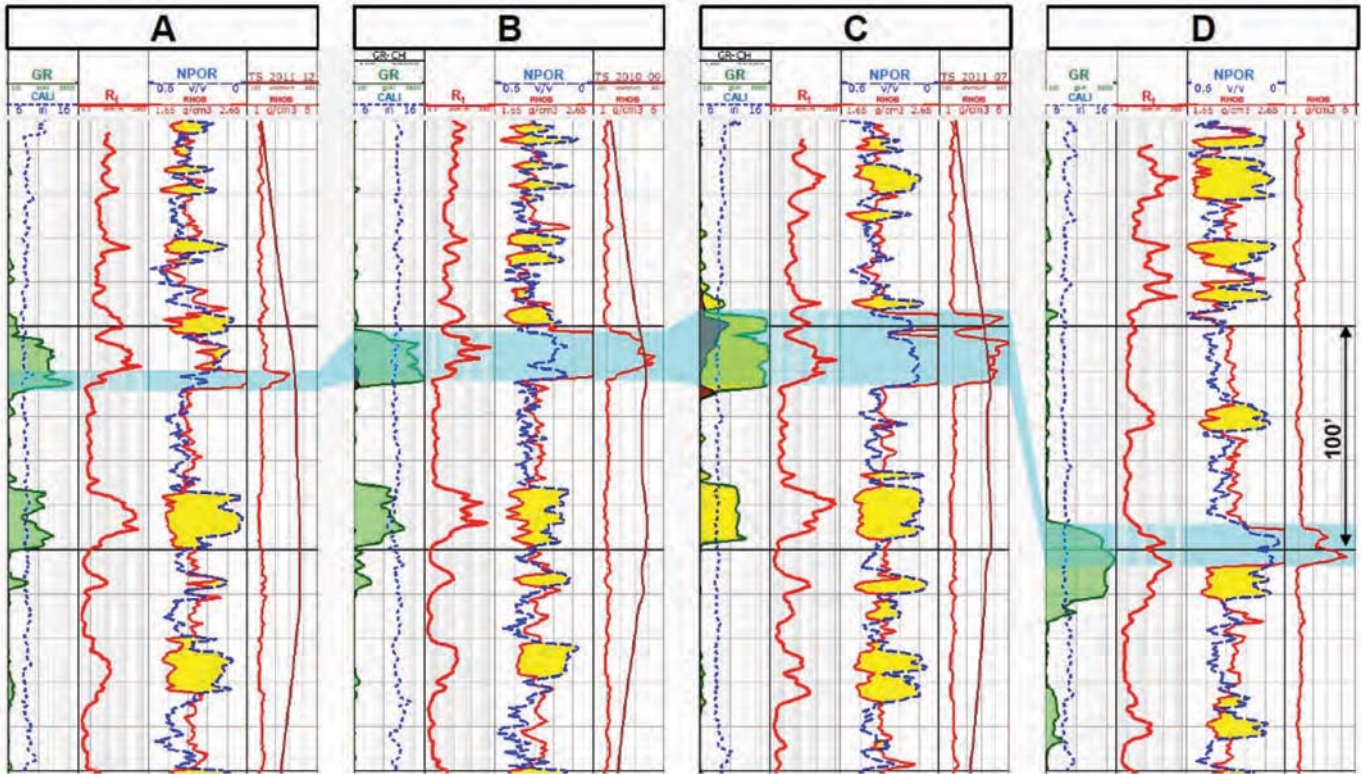


Fig. 5—Bulk-density values $>5 \text{ g/cm}^3$ (intervals in blue) are associated with GR readings $>5,000$ GAPI. Abrupt transitions, like those in Wells A and D, from extremely high bulk density to normal values in vapor-filled sands, are unlikely to occur in nature and suggest that the high bulk-density values are an artifact related to the high GR.

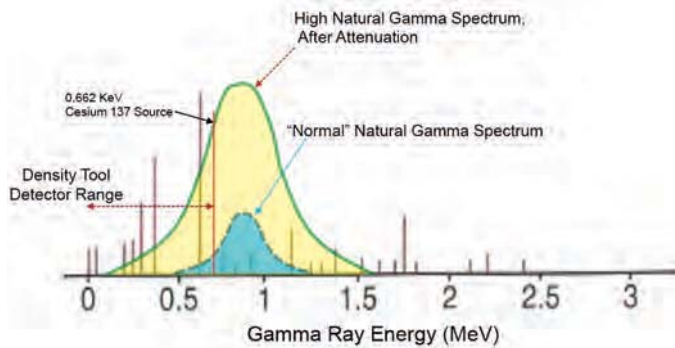


Fig. 6—The high apparent bulk-density values for the intervals in Fig. 5 occur when high natural gamma caused by CVG spills over into the density detector range, causing detector paralysis.

to be in the range of hundreds, not thousands, of GAPI units. This disconnection with the Midway-Sunset example suggests that, either the understanding of factors that affect CVG is flawed (and a new theory is required), or perhaps, there is an extraneous source of light hydrocarbon.

SPATIAL AND TEMPORAL CORRELATION

With thousands of wells to evaluate, a strategy was

developed to provide an overview of changes in CVG with time. For wells with intervals where GR readings >300 GAPI, Fig. 8 is a crossplot of the average GR value vs. time. Symbol size increases with net thickness exceeding the cutoff, for a range from 40 to 320 ft. The color of the data points varies strictly with the average GR value (y-axis).

Two episodes where GR readings increases above 1,000 GAPI are marked by the rectangles in Fig. 8. The first occurs during peak development of these heavy-oil sands from 1981 to 1990. The second, with considerably higher GR values, includes the wells in Fig. 7, and occurs after 1996. The cause of the high GR values during the second episode is not known, but it coincides with an increase in development activity for a deeper reservoir that contains lighter oil. The oil in this diatomite reservoir shares the same Monterey Formation source as the Tulare heavy oil (Hein, 2013), so these reservoirs are in communication. Low reservoir pressure in the Tulare, at the end of the steamflood development, could provide a mechanism allowing light oil (with high vapor pressure) from the diatomite to flow into the Tulare and increase CVG amplitude.

In order to visualize how CVG evolved with time, bubble maps were created (Figs. 9 and 10) for the area of

interest in Belridge Field. Each map shows all the wells that were drilled during a four-year time slice, starting with the wells drilled in 1980–1984 (i.e. 1 January 1980 to 31 December 1983). The legend shows how the color of the bubbles is related to the top depth of the first interval that has GR values >665 GAPI (CVG top depth). The size of the bubble is related to the product of the net thickness exceeding a 665 GAPI cutoff, and the average GR value for the net divided by 1,000 (CVG intensity). For example, a 33-ft interval, with average GR values of 10,000 GAPI would be represented by the largest bubble. Wells that do not have any intervals exceeding the cutoff are plotted as dots on the map.

The four maps in Fig. 9 show much less activity than those in Fig. 10. This is because fewer wells were drilled during 1980–1996, and also because CVG intensity is relatively low, where it does develop. The low CVG from 1980–1996 is consistent with steamflood of a well-sorted heavy-oil reservoir (Fig. 2).

After 1996, the bubble maps in Fig. 10 show areas where CVG increases significantly, for example, Areas A, B, and C. This observation is consistent with the increase in Fig. 8, but the maps show that there are localized clusters of wells where CVG develops.

If migration of light hydrocarbons from a deeper reservoir is responsible for the increase in CVG, then, for similar development methods and random well placement, localized CVG would suggest that migration pathways are a controlling factor. In reality, reservoir development methods vary over time, they also vary aerially and by reservoir, and new wells are not distributed evenly. Some areas of the deeper diatomite reservoir are developed by waterflood, for example, and others are developed by steamflood. Steam injection continues in parts of the Tulare reservoir. This mixture of activities makes it difficult to pinpoint the cause of variations in CVG.

Direct sampling and analysis of fluids from high CVG intervals, and continuous, in-situ observation of temperature,

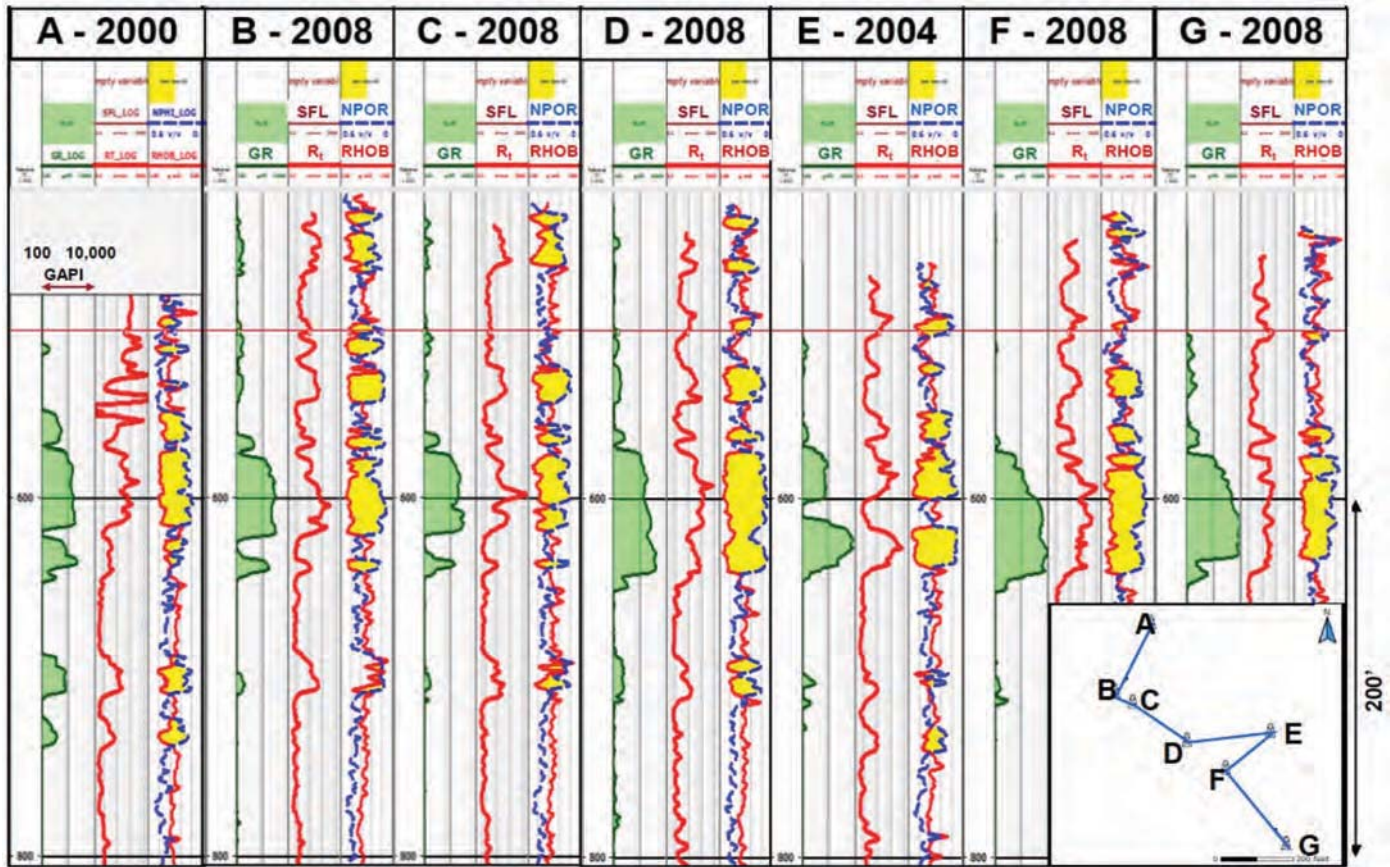


Fig. 7—Cross section for an area of Belridge Field including wells with high GR values (log scale from 100 to 10,000 GAPI). According to CVG theory, GR values are expected to be <1,000 GAPI for this steamflooded clean sand with low remaining oil saturation. The best explanation for the high GR values is that light hydrocarbons, sourced from the underlying Monterey Formation, overprint this reservoir.

pressure and CVG amplitude changes are needed to unravel the connection between CVG, migration pathways and development activities. Even with the challenges, systematic variations in CVG amplitude have been observed and can be used to constrain the possible explanations.

Area C (red polygon in Fig. 10) provides one example. CVG in this area becomes fully developed in 2004–2008, but there are indications of CVG before and after this time period.

Figure 11 is a cross section through wells in Area C, where CVG amplitude can exceed 10,000 GAPI through the zone of interest between 320 and 420 ft. The scale for the log display is at bottom left of the figure (Note: GR scales are linear 0 to 200 and logarithmic 200 to 20,000; the blue lines represent 1,000 and 10,000 GAPI, with yellow shading above 200 GAPI and red shading above 1,000 GAPI).

Of the seven wells shown in Fig. 11, four were drilled in January 2008, and three (A, D, and G) were drilled in 2012. All wells were drilled through the Tulare, to develop the deeper Monterey reservoir. At the time they were drilled, the Tulare steamflood in this area was done, and the vapor-filled reservoir was at a temperature close to 250°F.

The inset shows that the cross section is oriented NW-SE, parallel to the depositional shoreline of Lake Tulare. Well A is offset from the trendline of the other wells by about 50 ft to the southwest. In this well, the sand at 350

ft is thinner, as a result of a stratigraphic change or a fault. CVG amplitude in this well is about 200 GAPI—a typical value for a well-sorted heavy-oil sand, but dramatically lower than the 3,000 GAPI seen 50 ft away, in Well B. The best explanation for these observations is that, for this sand, there is a discontinuity between Wells A and B, and the light hydrocarbon vapor responsible for the high GR values in Well B is absent in Well A.

A less likely explanation for the absence of CVG in Well A is that CVG response decreased significantly from 2008, when Well B was drilled, to 2012, when Well A was drilled. Some support for this explanation is provided by the comparing the CVG in the 2012 Wells D and G, to the adjacent Wells E and F. From 2008 to 2012, CVG for these wells dropped by a factor of 10x from 10,000 GAPI to about 1,000 GAPI.

This explanation shows that CVG can change systematically with time, but CVG amplitude in Well A, at 100 GAPI, is still too low to be in equilibrium with Wells D and G. The conclusion that Sand A is isolated from the other sands remains valid but reservoir continuity is not the most interesting application of CVG.

Instead, the 10x decrease in CVG amplitude for 2008 to 2012 suggests that CVG is sensitive to vapor properties and that something, as yet unknown, caused the vapor to change.

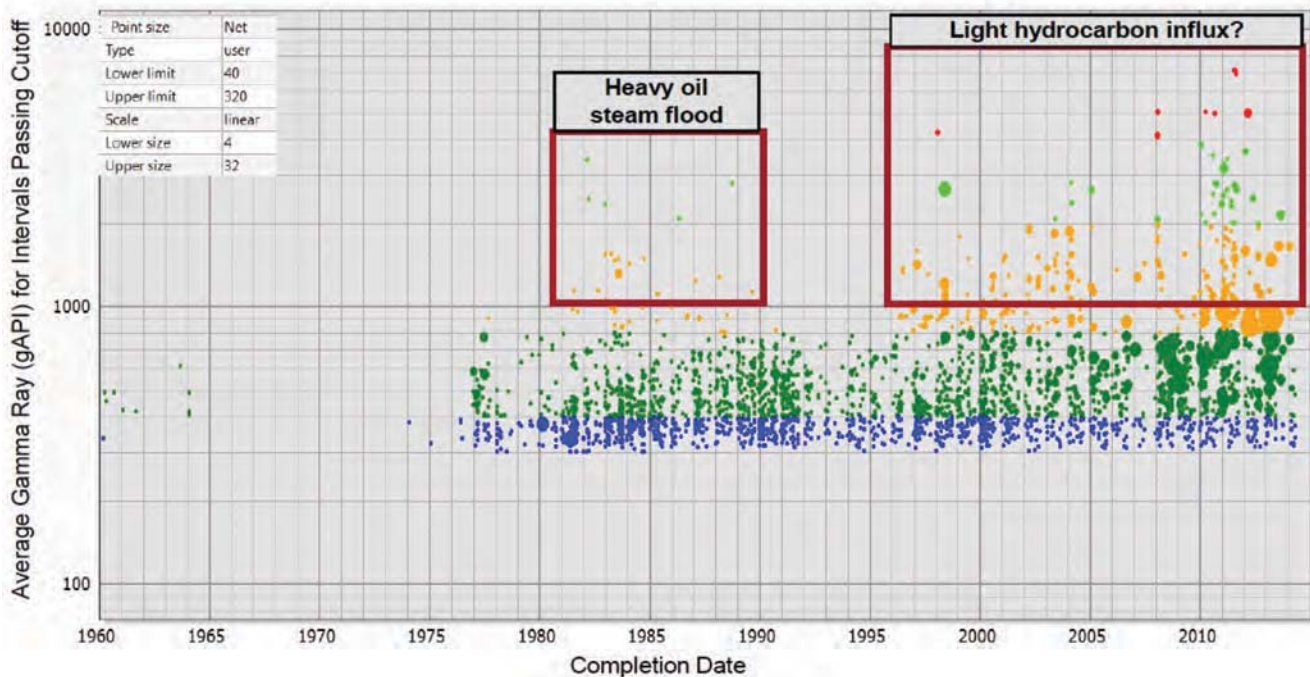


Fig. 8—Average GR values for new wells drilled from 1960–2015 for intervals with GR values exceeding a cutoff of 300 GAPI. Point size (area) is linearly related to the net thickness exceeding the cutoff, color is directly tied to the average GR value. Rectangles delineate the time frames and variations in high GR values for wells that were part of (1) the original heavy-oil steamflood, and (2) a second event that increased GR values through the vapor-filled sands that remain as the steamflood comes to an end.

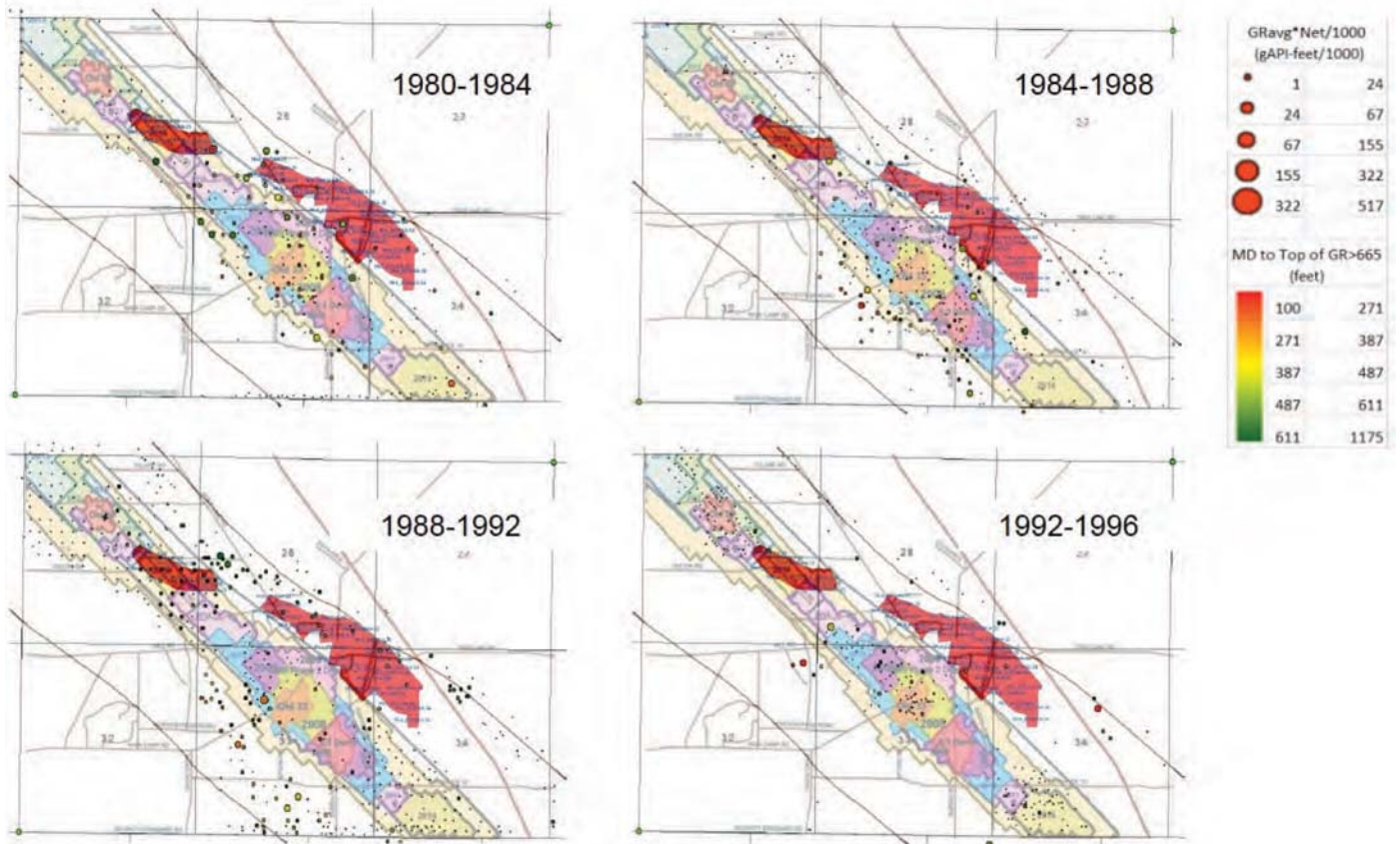


Fig. 9—Bubble maps for time slices including wells drilled from 1980-1996. The legend shows that point size (area) is linearly related to the product of net thickness exceeding a cutoff of 665 GAPI multiplied by the average GR value for those intervals divided by 1,000. Point color is tied to the depth of the shallowest interval passing the cutoff.

The change is uncorrelated with any other log response, and suggests that CVG provides a unique new capability for vapor characterization.

CONCLUSIONS

CVG temporarily concentrates naturally occurring radon downhole, around a chilled wellbore. The effect has only been observed in the vapor cloud that remains after steamflood development of heavy-oil reservoirs, however, it may be possible to generate CVG in other contexts. CVG values are higher in poorly sorted rocks with higher remaining oil saturation because radon solubility is higher in oil than water. Very high GR values >20,000 GAPI, are likely to be associated with light hydrocarbon vapor that has higher vapor pressure than water at temperatures of 100 to 150°C (212 to 302°F).

CVG is a sensitive measurement with high signal-to-noise ratio, and coherent spatial and temporal variations. Patterns of CVG amplitude variations suggest that it reflects

reservoir fluid property changes.

Additional work will lead to a more complete understanding of CVG and how it can be used to improve reservoir characterization and process surveillance. Specifically, fluids that generate CVG need to be sampled and analyzed. Laboratory work is needed to quantify the relationship between CVG amplitude and vapor characteristics, and continuous monitoring of CVG in observation wells is needed to understand and test the responsiveness of CVG to development activities.

ACKNOWLEDGEMENTS

The author is grateful to Aera Energy LLC, Dan Rayes, Saul Hernandez and Harold Orndorff for supporting this project, and to John Magee, Alfredo Urdaneta, Don Deininger, Darwin Ellis and Oliver Mullins for their interest, inspiration and ongoing discussions on CVG.

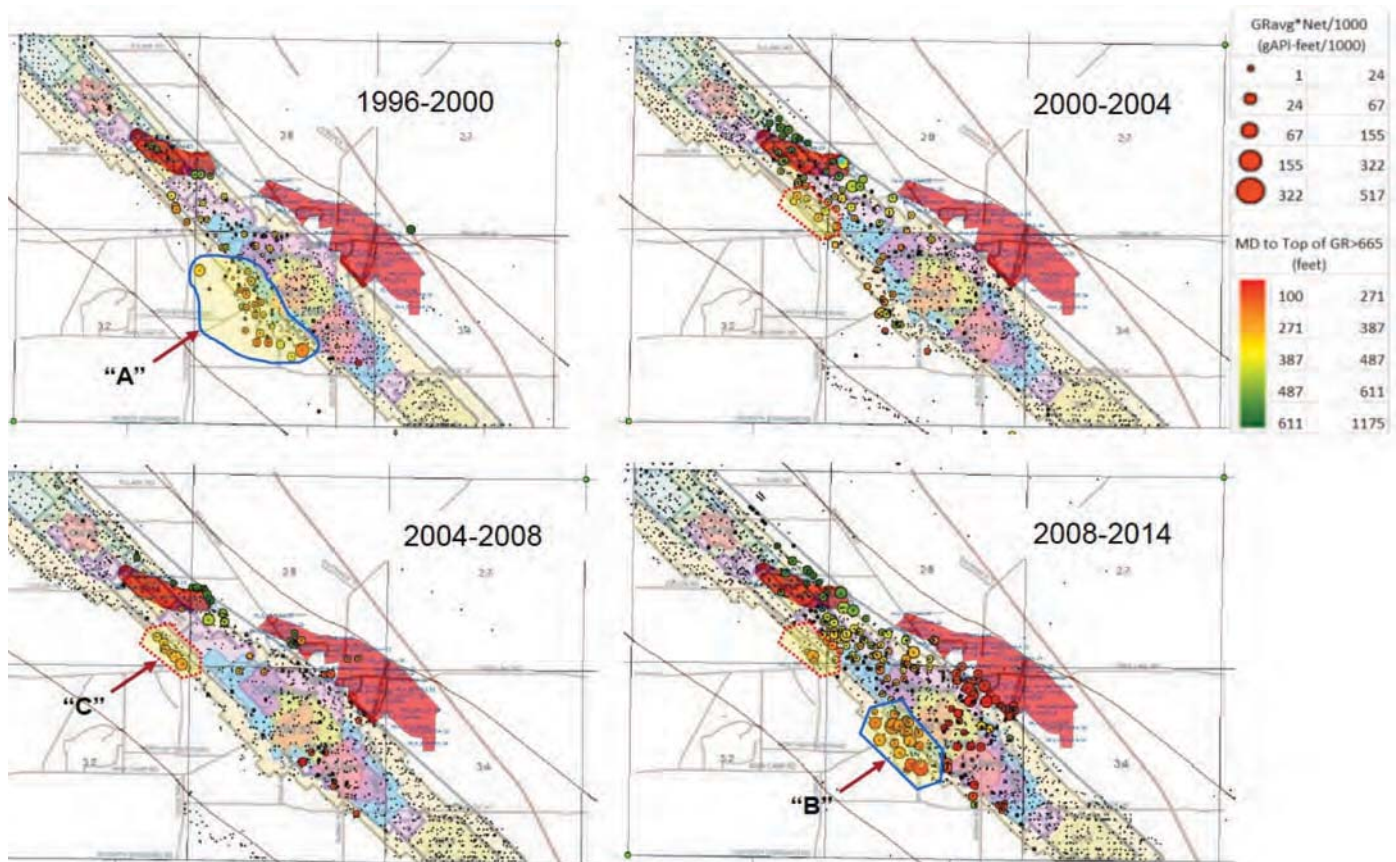


Fig. 10—Bubble maps for time slices including wells drilled from 1996-2014. The legend shows that point size (area) is linearly related to the product of net thickness exceeding a cutoff of 665 GAPI multiplied by the average GR value for those intervals divided by 1,000. Point color is tied to the depth of the shallowest interval passing the cutoff. Areas A, B and C show interesting CVG development that appears to occur through specific time periods.

REFERENCES

- Al-Azmi, D., Snopek, D., Sayed, A.M., and Domanski, T., 2004, A Simple Bubbling System for Measuring Radon (^{222}Rn) Gas Concentrations in Water Samples Based on the High Solubility of Radon in Olive Oil, *Journal of Environmental Radioactivity*, **71**(2), 175–186.
- Battino, R., and Clever, H.L., 1966, The Solubility of Gases in Liquids, *Chemical Reviews*, **66**(4), 395–463. DOI: 10.1021/cr60242a003.
- Ellis, D.V., 2013, Personal Communication: Unusual Log Response in 588ZR2-29 and 933PR-33 - Could the Density Gamma Detectors Stop Working?
- Gross, K., and Markun, F., 1999, Fluid-Based System for Radon Mitigation, Paper 1999-09 presented at the 1999 International Radon Symposium, Las Vega, Nevada, USA. https://www.aarst.org/proceedings/1999/1999_09_Fluid-Based_System_For_Radon_Mitigation.pdf. Accessed August 12, 2015.
- Hein, F.J., 2013, Overview of Heavy Oil, Seeps, and Oil (Tar) Sands, California, in Hein, F.J., Leckie, D., Larter, S., and Suter, J.R., editors, *Heavy-Oil and Oil-Sand Petroleum Systems in Alberta and Beyond*, AAPG Studies in Geology **64**, 407–435.
- Kharaka, Y.K., and Specht, D.K., 1988, The Solubility of Noble Gases in Crude Oil at 25–100°C, *Applied Geochemistry*, **3**, 137–144.
- O'Sullivan, T.P., 2008, High Gamma Radiation in Heavy-Oil Steam Zones: A Condensation-Induced Effect, Paper N, *Transactions, SPWLA 49th Annual Logging Symposium*, Edinburgh, Scotland, UK, 25–28 May.
- O'Sullivan, T.P., 2009, Condensation-Induced Gamma Radiation as a Method for the Identification of Condensable Vapor, U.S. Patent No. 7,538,318, May 26, 2009.
- UNSCEAR, 1982, Exposures to Radon and Thoron and Their Decay Products, Report to the General Assembly, Annex D, 141–210, Table 2, Properties of Radon, United Nations, New York. http://www.unscear.org/docs/reports/1982/1982-D_unscear.pdf. Accessed August 12, 2015.

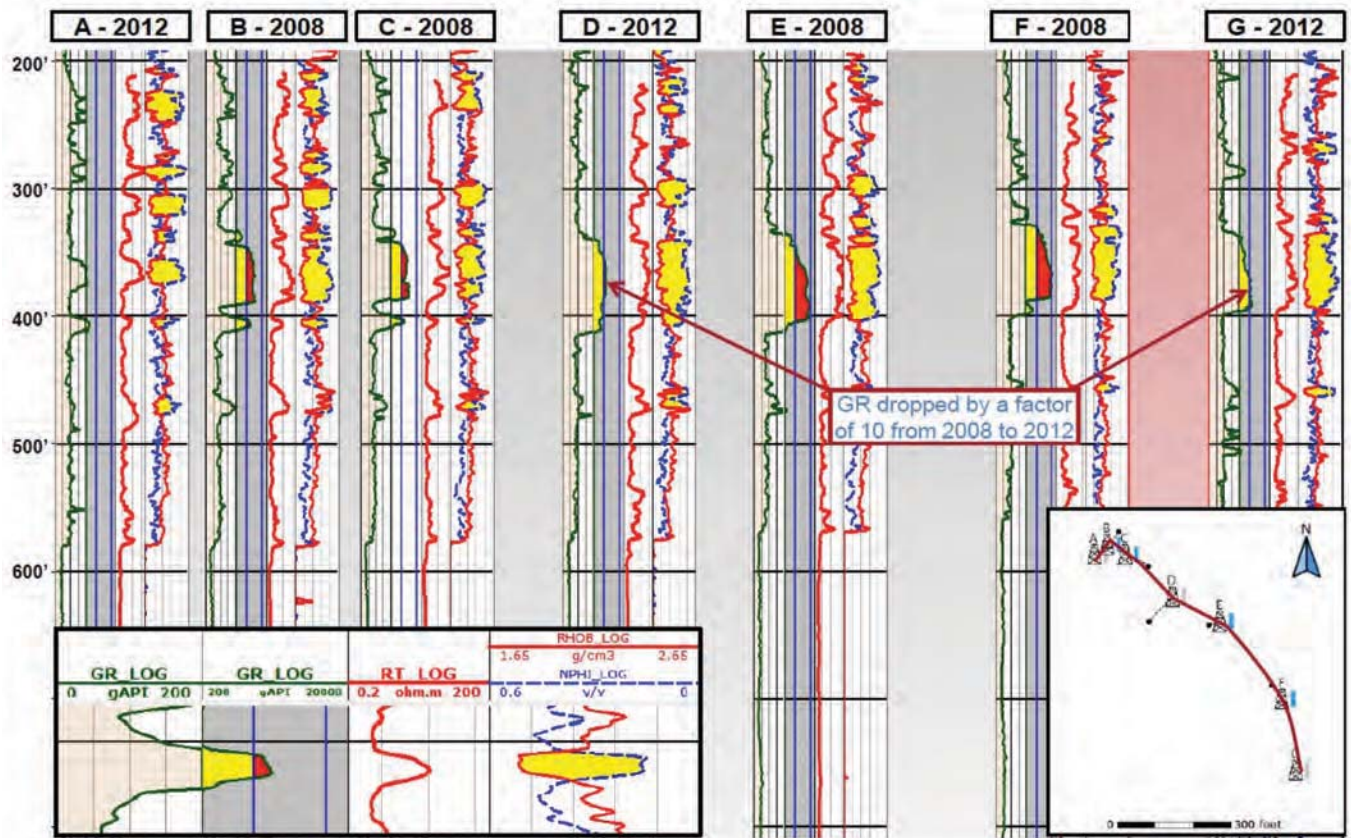


Fig. 11—Cross section for wells in Area C, showing good lateral correlation of high CVG, approaching 10,000 GAPI in Wells E and F. Wells D and G, drilled in 2012, have lower GR values than surrounding wells, probably because the vapor cloud characteristics changed from 2008-2012. Inset at lower left provides details on curve scales and colors.

ABOUT THE AUTHOR



Terry O'Sullivan is a technical consultant for Aera Energy LLC, in Bakersfield, California, where he has focused on heavy-oil reservoirs since 1997. Prior to that, he was with Ampolex, in Perth, Australia; Maxus SES, in Jakarta, Indonesia; Unocal, in California; and Exxon, in Texas; where he worked on a variety of exploration and development projects.